PHILOSOPHICAL TRANSACTIONS OF THE ROYAL SOCIETY A MATHEMATICAL, PHYSICAL & ENGINEERING SCIENCES

Weak localization in monolayer and bilayer graphene

D.W Horsell, F.V Tikhonenko, R.V Gorbachev and A.K Savchenko

Phil. Trans. R. Soc. A 2008 **366**, 245-250
doi: 10.1098/rsta.2007.2159

PHILOSOPHICAL TRANSACTIONS OF THE ROYAL SOCIETY A

Phil. Trans. R. Soc. A (2008) **366**, 245–250
doi:10.1098/rsta.2007.2159
Published online 19 November 2007

Weak localization in monolayer and bilayer graphene

By D. W. Horsell, F. V. Tikhonenko, R. V. Gorbachev and A. K. Savchenko*

School of Physics, University of Exeter, Stocker Road, Exeter EX4 4QL, UK

We demonstrate quantitative experimental evidence for a weak localization correction to the conductivity in monolayer and bilayer graphene systems. We show how inter- and intra-valley elastic scattering control the correction in small magnetic fields in a way which is unique to graphene. A clear difference in the forms of the correction is observed in the two systems, which shows the importance of the interplay between the elastic scattering mechanisms and how they can be distinguished. Our observation of the correction at zero-net carrier concentration in both systems is clear evidence of the inhomogeneity engendered into the graphene layers by disorder.

Keywords: quantum interference; graphene; weak localization

1. Introduction

Since the discovery that the atomically thin carbon allotrope 'graphene' could be fabricated as a field effect device (Novoselov *et al.* 2004), a great deal of interest in its properties has been generated. The two-dimensional charge carriers in graphene are distinct from those created in traditional, semiconductor-based systems due to the dispersion relation (linear at low energies for monolayer graphene and parabolic for bilayer) and carrier chirality. Scattering in graphene, and hence interference between the scattered charge carriers, is therefore highly unusual and can be observed in such effects as the weak localization (WL) correction to the conductivity.

It has become clear recently that WL in monolayer (Suzuura & Ando 2002; McCann *et al.* 2006; Tikhonenko *et al.* 2007) and bilayer (Gorbachev *et al.* 2007; Kechedzhi *et al.* 2007) graphene is in fact two, rather distinct effects. We therefore begin by describing the properties of these systems. As a result of two sublattices in graphene's honeycomb crystal structure, charge carriers take on the additional property of 'chirality' (defined by the 'pseudospin' quantum number) due to the reflectional symmetry of these sublattices. Graphene has two valleys in the first Brillouin zone (see figure 1, inset): the Berry phase of the pseudospin incurred by a carrier circumscribing one valley is π in the case of monolayer and 2π in the case of bilayer. Backscattering in the monolayer (half circumscription of the valley)

* Author for correspondence (a.k.savchenko@exeter.ac.uk).

One contribution of 11 to a Discussion Meeting Issue 'Carbon-based electronics: fundamentals and device applications'.

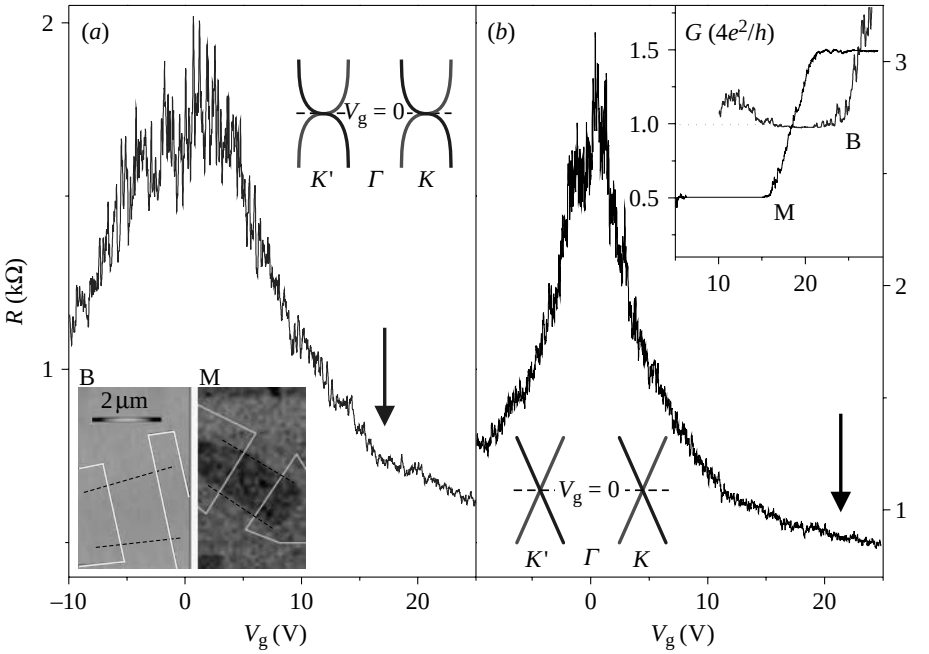

Figure 1. The dependence of the resistance on gate voltage for (*a*) bilayer (B) and (*b*) monolayer (M) graphene systems. The arrows indicate the high-concentration regions where the WL is studied. The bottom left inset shows optical and electron micrographs of B and M, respectively. The top right inset shows quantum Hall plateaux at 14 and 12 T for B and M, respectively. The line drawings illustrate the associated dispersion relations.

is therefore effectively suppressed as the two opposing interfering trajectories pick up a phase difference of π, giving rise to a positive correction to the conductivity. In contrast, in the bilayer backscattering is enhanced leading to a (conventional) negative correction. Thus, in monolayer graphene weak anti-localization (WAL) is expected to occur and in bilayer WL is expected.

In addition to conventional inelastic phase-breaking events, there are energy-conserving events that control the manifestation of WL in monolayer (McCann *et al.* 2006; Morozov *et al.* 2006; Heersche *et al.* 2007; Tikhonenko *et al.* 2007; Wu *et al.* 2007) and bilayer (Gorbachev *et al.* 2007; Kechedzhi *et al.* 2007) graphene. These are distinguished as chirality-breaking intra-valley scattering, inter-valley scattering and 'trigonal warping' effect. The last of these relates to the distortion of the dispersion relation at finite energy which leads to a suppression of WL (McCann *et al.* 2006). Additional suppression can occur from any chirality-breaking event within a valley, which can result from lattice distortions and dislocations, as well as ripples in the graphene membrane (Morpurgo & Guinea 2006). However, the possibility for carriers to scatter between two valleys coherently can negate these intra-valley effects and restore WL. This inter-valley scattering can occur off defects that are sharp on the scale of the lattice spacing, including the geometric boundaries. Such scattering can also break intra-valley chirality; however, by mixing the two valleys the effective symmetry of the Fermi surface and probability to conserve pseudospin are both increased.

The WL correction in monolayer $\delta\sigma_1$ (McCann *et al.* 2006) and bilayer $\delta\sigma_2$ (Kechedzhi *et al.* 2007) graphene is predicted to have the form

$$\frac{\pi\hbar}{e^2}\cdot\delta\sigma_{1(2)}(\mathrm{B}) = \mathcal{F}\left(\frac{\tau_\mathrm{B}^{-1}}{\tau_\varphi^{-1}}\right) - \mathcal{F}\left(\frac{\tau_\mathrm{B}^{-1}}{\tau_\varphi^{-1}+2\tau_i^{-1}}\right) \mp 2\mathcal{F}\left(\frac{\tau_\mathrm{B}^{-1}}{\tau_\varphi^{-1}+\tau_i^{-1}+\tau_*^{-1}}\right)$$

$$\equiv \mathcal{F}_1 - \mathcal{F}_2 \mp 2\mathcal{F}_3, \tag{1.1}$$

where $\mathcal{F}(x) = \ln(x) + \Psi(1/2+1/x)$, $\Psi(x)$ is the digamma function, $\tau_\mathrm{B}^{-1} = (4De/\hbar)\mathrm{B}$ and the negative and positive sign of $\mathcal{F}_3$ refers to the monolayer and bilayer, respectively. The rates τ_x^{-1} are associated with phase-breaking (φ), inter-valley (i) and intra-valley (*) scattering, where $\tau_*^{-1} = \tau_w^{-1} + \tau_z^{-1}$ and $\tau_{z,w}^{-1}$ are the single valley chirality-breaking and trigonal warping rates, respectively. In monolayers, if there is no intra- or inter-valley scattering ($\tau_\varphi^{-1} \gg \tau_i^{-1}, \tau_*^{-1}$) then full WAL ($\delta\sigma_1 = -2\mathcal{F}_3$) occurs. This localization is destroyed in the presence of intra-valley scattering ($\tau_*^{-1} \gg \tau_\varphi^{-1} \gg \tau_i^{-1}$) as $\mathcal{F}_3 \to 0$. However, if inter-valley scattering is possible ($\tau_*^{-1} \gg \tau_\varphi^{-1} \sim \tau_i^{-1}$) then WL occurs, although reduced by a factor of two compared with conventional WL ($\delta\sigma_1 \sim \mathcal{F}_1$). In bilayers, WL always occurs (due to the positive contribution of $\mathcal{F}_3$), but the shape of the resulting function is controlled by the scattering rates.

2. Experiment and results

We present here a quantitative study of WL in monolayer and bilayer systems. The graphene flakes were made by the method of mechanical exfoliation (Novoselov *et al.* 2004) and deposited on an n^+Si substrate covered by a 300 nm SiO_2 layer. Lithographically defined Au/Cr contacts were subsequently made to each flake. The carrier density was controlled by a gate voltage applied between the n^+Si and the graphene. Two rectangular samples shown in figure 1*a* (inset) will be discussed: bilayer B of width $W = 1.8\,\mu\mathrm{m}$ and length $L = 1.5\,\mu\mathrm{m}$ and monolayer M with $W = L = 1.3\,\mu\mathrm{m}$.

Figure 1 shows the resistance as a function of gate voltage for both samples. A peak is seen at $V_\mathrm{g} = 0$, the 'electroneutrality' point, where the charge carriers change from holes to electrons. Mobilities of the two samples away from the electroneutrality point are 8000 and 5000 $\mathrm{cm^2\,V^{-1}\,s^{-1}}$ for B and M, respectively (and corresponding contact resistances are 175 and 400 Ω). Mesoscopic fluctuations are also seen due to the small sizes of the samples with respect to the phase-breaking length (Gorbachev *et al.* 2007; Tikhonenko *et al.* 2007) and these decrease with increasing temperature. The inset data show the quantum Hall plateaux measured for each sample and the expected difference of half of a resistance quantum ($h/4e^2$ for graphene) between the systems is clearly seen. The correction to the conductivity due to WL is measured by the procedure given by Gorbachev *et al.* (2007) where, to negate the fluctuations, $\delta\sigma$ is averaged over a gate voltage window, $\Delta V_\mathrm{g} = 2\mathrm{V}$: $\delta\sigma = \langle\sigma(\mathrm{B}, V_\mathrm{g}) - \sigma(0, V_\mathrm{g})\rangle_{\Delta V_\mathrm{g}}$.

Figure 2 shows the effect of magnetic field on the conductivity of samples B and M both in the high electron concentration region ($n \sim 1.5\times10^{12}\,\mathrm{cm^{-2}}$) and the electroneutrality region. The form of this correction is described well by equation (1.1). All parameters determined from fits to this equation are temperature independent below $T \sim 3\,\mathrm{K}$, and here we focus only on these

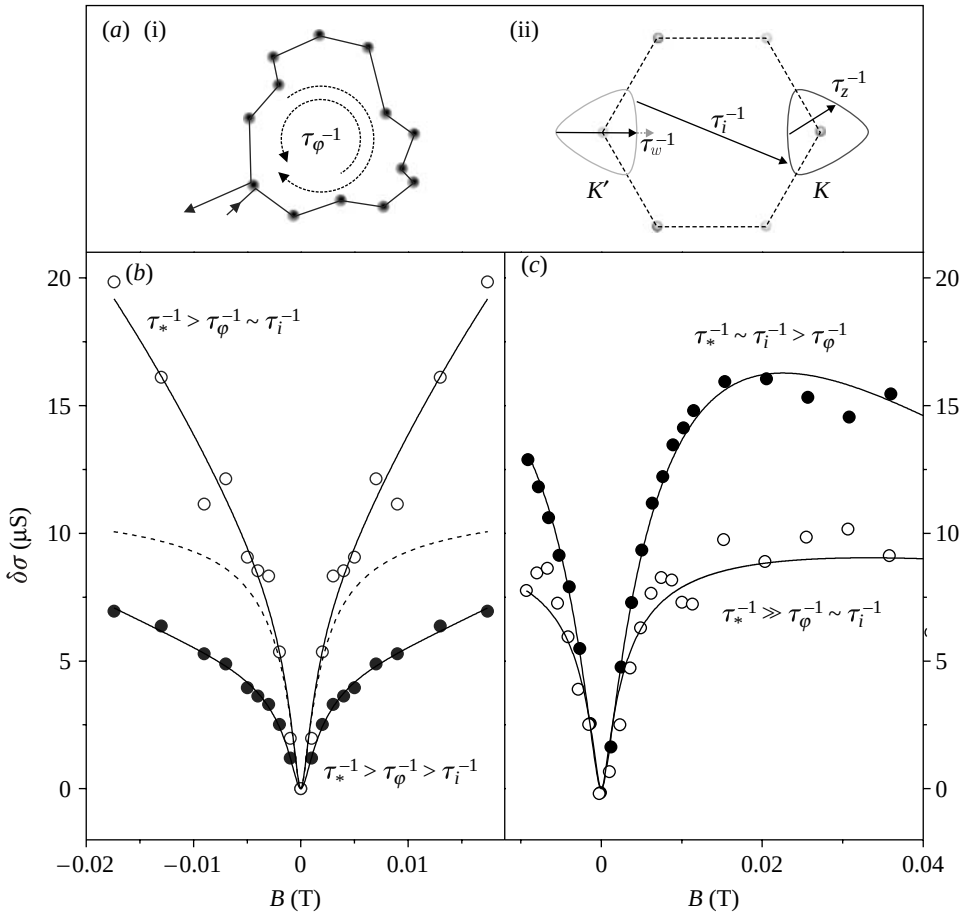

Figure 2. (*a*) Illustration of the rates that control the WL in graphene. (i) A real space diagram of the closed trajectories responsible for the effect, which are limited in size by the dephasing rate τ_φ^{-1}. (ii) The shape of the Fermi surface at finite energy, illustrating the processes responsible for trigonal warping (τ_w^{-1}), chirality-breaking (τ_z^{-1}) and inter-valley scattering (τ_i^{-1}). (*b*,*c*) The correction to the conductivity for samples (*b*) B and (*c*) M as a function of magnetic field in the electroneutrality (filled circles) and high carrier concentration (empty circles) regions. The data are shown together with the best fit (solid lines) by equation (1.1). In (*b*), the dashed line represents the case when $\tau_*^{-1} \gg \tau_\varphi^{-1} \sim \tau_i^{-1}$.

T-independent values (the *T* dependence of the phase-breaking rate τ_φ at higher temperatures is discussed elsewhere by Gorbachev *et al.* (2007) and Tikhonenko *et al.* (2007)).

In figure 2*b*,*c* we see a striking difference between the WL in samples B and M. Let us first look at the fitting of $\delta\sigma$(B) to equation (1.1) at high carrier concentration (empty circles). For both samples, a reasonable fit is achieved if $\mathcal{F}_3$ is suppressed by strong intra-valley scattering ($\tau_*^{-1} \to \infty$). (In the theories by McCann *et al.* (2006) and Kechedzhi *et al.* (2007), the momentum relaxation rate τ_{p}^{-1} represents fast, pseudospin-conserving events and hence the upper limit of τ_*^{-1} must inherently be τ_{p}^{-1}.) The fact that we have WL rather than WAL in sample M requires $\tau_*^{-1} \gg \tau_\varphi^{-1} \sim \tau_i^{-1}$ which indeed we see in the fit: $\tau_\varphi^{-1} = 0.083$,

$\tau_i^{-1} = 0.056$ and $\tau_*^{-1} = 12\ \mathrm{ps}^{-1}$. Our estimation for τ_p^{-1} in the same gate voltage region is $13\ \mathrm{ps}^{-1}$. As $\tau_i^{-1} \approx \tau_\varphi^{-1}$, $\delta\sigma_1 = \mathcal{F}_1 - \mathcal{F}_2$ and we should expect a WL that tends to saturate at higher magnetic fields as seen in the figure ($\tau_i^{-1} \approx \tau_\varphi^{-1}$ because both are limited by the size of the sample; Tikhonenko *et al.* 2007).

For the bilayer, the fit gives $\tau_\varphi^{-1} = 0.029$, $\tau_i^{-1} = 0.021$ and $\tau_*^{-1} = 0.38\ \mathrm{ps}^{-1}$. Since the phase-breaking rate in the bilayer is one-third of that in the monolayer, the range of fields over which $\delta\sigma$ is considered is scaled accordingly to give equivalent scales in τ_B^{-1}. Therefore, since τ_i^{-1} in the samples is different by the same factor as τ_φ^{-1}, the only reason for the enhancement of the WL correction in the bilayer over that of the monolayer lies in its smaller rate τ_*^{-1} that augments the contribution of term $\mathcal{F}_3$. We can see the effect the third term has by removing it (setting $\tau_*^{-1} = \infty$): this is shown by the dashed line in figure 2*b*, which is almost identical to the functional form of the WL in the monolayer.

The fact that WL is seen in the electroneutrality region of both samples, figure 2*b*,*c* (filled circles), is currently somewhat of a conundrum. The reason is generally ascribed to the formation of electron–hole puddles (Gorbachev *et al.* 2007). When we compare bilayer and monolayer systems, in the former $\delta\sigma(\mathrm{B})$ is found to be suppressed in the electroneutrality region whereas in the latter it is enhanced. In the bilayer, $\tau_\varphi^{-1} = 0.022$, $\tau_i^{-1} = 0.007$ and $\tau_*^{-1} = 0.71\ \mathrm{ps}^{-1}$. The decrease of τ_i^{-1} (accompanied by negligible change in τ_φ^{-1}) is the important factor here, as suppression of the WL in the bilayer can only be a result of term $\mathcal{F}_2$. In contrast, in the monolayer the enhanced WL at low fields is followed by a distinct downturn at higher fields (continuing beyond the range shown). The fit to equation (1.1) gives $\tau_\varphi^{-1} = 0.23$ and $\tau_i^{-1} = \tau_*^{-1} = 1.6\ \mathrm{ps}^{-1}$. (A good fit is possible for $\tau_*^{-1} \to 0$; however, we note that our choice of fit with $\tau_i^{-1} = \tau_*^{-1}$ represents a physical limit as any inter-valley scattering will necessarily limit intra-valley scattering.) This strong enhancement of the inter-valley scattering, accompanied by a suppression of the intra-valley scattering, makes $\mathcal{F}_3$ a significant term and also weakens the second term. This results in the enhancement and downturn of the WL in the electroneutrality region of sample M seen in the figure.

3. Discussion

From the above analysis, we attempt to consolidate our findings as follows. In the bilayer, τ_*^{-1} remains unchanged between the high-concentration and electroneutrality regions. (The momentum relaxation rate, however, increases by an order of magnitude outside the electroneutrality region.) As trigonal warping is expected to strongly depend on carrier concentration, intra-valley scattering in the bilayer therefore appears to be limited by chirality-breaking scattering from dislocations and ripples which depend little on concentration. The suppression of inter-valley scattering in the electroneutrality region is currently not understood: as the density of states is constant in a bilayer system and the number of atomically sharp impurities also remains fixed it must be the result of inhomogeneity in the system (electron–hole puddles) that acts to screen some of the impurities.

In the monolayer, τ_*^{-1} has a strong dependence on concentration (much stronger than the corresponding twofold change in τ_p^{-1}) and could result from trigonal warping, where it is predicted by McCann *et al.* (2006) that $\tau_w^{-1} \propto \tau_\mathrm{p} n^2$.

An increase of inter-valley scattering in the electroneutrality region can be the result of poorer screening, as the screening is not as effective in the monolayer as it is in the bilayer.

4. Conclusion

In conclusion we have shown that WL exists in monolayer and bilayer graphene systems for the case of a large and zero-net carrier concentration. We have shown the importance of the elastic (intra- and inter-valleys) scattering mechanisms and how they appear directly in the form of the positive magnetoconductance.

References

Gorbachev, R. V., Tikhonenko, F. V., Mayorov, A. S., Horsell, D. W. & Savchenko, A. K. 2007 Weak localization in bilayer graphene. *Phys. Rev. Lett.* **98**, 176805. (doi:10.1103/PhysRevLett.98.176805)

Heersche, H. B., Jarillo-Herrero, P., Oostinga, J. B., Vandersypen, L. M. K. & Morpurgo, A. F. 2007 Bipolar supercurrent in graphene. *Nature* **446**, 56–59. (doi:10.1038/nature05555)

Kechedzhi, K., Fal'ko, V. I., McCann, E. & Altshuler, B. L. 2007 Influence of trigonal warping on interference effects in bilayer graphene. *Phys. Rev. Lett.* **98**, 176806. (doi:10.1103/PhysRevLett.98.176806)

McCann, E., Kechedzhi, K., Fal'ko, V. I., Suzuura, H., Ando, T. & Altshuler, B. L. 2006 Weak-localization magnetoresistance and valley symmetry in graphene. *Phys. Rev. Lett.* **97**, 146805. (doi:10.1103/PhysRevLett.97.146805)

Morozov, S. V., Novoselov, K. S., Katsnelson, M. I., Schedin, F., Ponomarenko, L. A., Jiang, D. & Geim, A. K. 2006 Strong suppression of weak localization in graphene. *Phys. Rev. Lett.* **89**, 016801. (doi:10.1103/PhysRevLett.97.016801)

Morpurgo, A. F. & Guinea, F. 2006 Intervalley scattering, long-range disorder, and effective time-reversal symmetry breaking in graphene. *Phys. Rev. Lett.* **97**, 196804. (doi:10.1103/PhysRevLett.97.196804)

Novoselov, K. S., Geim, A. K., Morozov, S. V., Jiang, D., Zhang, Y., Dubonos, S. V., Grigorieva, I. V. & Firsov, A. A. 2004 Electric field effect in atomically thin carbon films. *Science* **306**, 666–669. (doi:10.1126/science.1102896)

Suzuura, H. & Ando, T. 2002 Crossover from symplectic to orthogonal class in a two-dimensional honeycomb lattice. *Phys. Rev. Lett.* **89**, 266603. (doi:10.1103/PhysRevLett.89.266603)

Tikhonenko, F. V., Horsell, D. W., Gorbachev, R. V. & Savchenko, A. K. 2007 Weak localisation in graphene flakes. (http://arxiv.org/abs/0707.0140)

Wu, X., Li, X., Song, Z., Berger, C. & de Heer, W. A. 2007 Weak antilocalization in epitaxial graphene: evidence for chiral electrons. *Phys. Rev. Lett.* **98**, 136801. (doi:10.1103/PhysRevLett.98.136801)